Cadherin-2 participates in the morphogenesis of the zebrafish inner ear

Sherry Babb-Clendenon[1,*], Yu-chi Shen[2,*], Qin Liu[3], Katharyn E. Turner[1], M. Susan Mills[1], Greg W. Cook[1], Caroline A. Miller[4], Vincent H. Gattone, II[4], Kate F. Barald[2] and James A. Marrs[1,†]

[1]Department of Medicine, Indiana University Medical Center, 950 West Walnut Street, Indianapolis, IN 46202, USA
[2]Department of Cell and Developmental Biology, University of Michigan, Ann Arbor, MI 48109-0616, USA
[3]Department of Biology, University of Akron, Akron, OH 44325
[4]Department of Anatomy, Indiana University Medical Center, Indianapolis, IN 46202

*These authors contributed equally to this manuscript.
†Author for correspondence (e-mail: jmarrs@iupui.edu)

Accepted 12 October 2006
Journal of Cell Science 119, 5169-5177 Published by The Company of Biologists 2006
doi:10.1242/jcs.03299

Summary

Molecular mechanisms that control inner ear morphogenesis from the placode to the three-dimensional functional organ are not well understood. We hypothesize that cell-cell adhesion, mediated by cadherin molecules, contributes significantly to various stages of inner ear formation. Cadherin-2 (Cdh2) function during otic vesicle morphogenesis was investigated by examining morpholino antisense oligonucleotide knockdown and *glass onion* (*glo*) (Cdh2 mutant) zebrafish embryos. Placode formation, vesicle cavitation and specification occurred normally, but morphogenesis of the otic vesicle was affected by Cdh2 deficiency: semicircular canals were reduced or absent. Phalloidin staining of the hair cell stereocillia demonstrated that *cadherin-2* (*cdh2*) loss-of-function did not affect hair cell number, but acetylated tubulin labeling showed that hair cell kinocilia were shorter and irregularly shaped. Statoacoustic ganglion size was significantly reduced, which suggested that neuron differentiation or maturation was affected. Furthermore, *cdh2* loss-of-function did not cause a general developmental delay, since differentiation of other tissues, including eye, proceeded normally. These findings demonstrate that Cdh2 selectively affects epithelial morphogenetic cell movements, particularly semicircular canal formation, during normal ear mophogenesis.

Supplementary material available online at
http://jcs.biologists.org/cgi/content/full/119/24/5169/DC1

Key words: N-cadherin, Zebrafish, Ear development, Morphogenesis, Antisense oligonucleotide

Introduction

The vestibular apparatus in the vertebrate inner ear detects linear acceleration and gravitation, which allows the animal to maintain its orientation in three-dimensional space. The inner ear also detects sound through the cochlea or equivalent structures. Both the vestibular and auditory portions of the ear contain sensory cells called hair cells. Hair cells and their associated supporting cells differentiate from the otic vesicle epithelium. Hair cells elaborate a bundle of modified, actin-cored microvilli called stereocilia and a single modified, 9+2 microtubule, primary cilium, termed the kinocilium. The inner ear forms through a series of developmental events that include otic placode induction and condensation, otic vesicle lumen formation (cavitation in fish and frogs), differentiation of sensory patches (containing hair cells and their underlying supporting cells), statoacoustic ganglion delamination and development, and semicircular canal morphogenesis (Barald and Kelley, 2004). Molecular mechanisms that regulate these events are the focus of intense study but remain poorly understood. The zebrafish has become an important genetic model organism, which is amenable to genetic analysis of ear development (Whitfield et al., 1996; Ernest et al., 2000; Whitfield et al., 2002; Liu et al., 2003; Nicolson, 2005), including the role of cadherin-23 in mechanotransduction of sound (Sollner et al., 2004; Nicolson, 2005). We have initiated a series of studies to evaluate the contribution of cadherin cell-cell adhesion function to zebrafish inner ear development (Novince et al., 2003).

Cadherins are homotypic cell adhesion molecules that were identified as regulators of morphogenesis, mediating cell migration and cell shape changes, which lead to tissue shape changes and other morphogenetic processes (Gumbiner, 2005). Cadherin-1 knockdown and *half baked* mutant zebrafish embryos display significant defects in ectodermal cell migration and cell shape changes during epiboly and gastrulation (Babb and Marrs, 2004; Kane et al., 2005; Montero et al., 2005; Shimizu et al., 2005). We previously demonstrated that inhibiting cadherin function in MDCK cells affects morphogenesis in three-dimensional cyst cultures (Troxell et al., 2001), which shows that cadherin adhesion helps to regulate epithelial morphogenesis.

Cadherin adhesion molecules also regulate cell differentiation events that generate various cell types in a tissue. For example, the most notable defect we found in our analysis of the visual system of cadherin-4 knockdown zebrafish embryos was a failure of the neural retina to execute the neurogenic wave of differentiation (Babb et al., 2005). Differentiation of inner ear cells, including the hair cells,

Table 1. Loss of Cdh2 does not affect hair cell number

Hair cell number		Average	s.d.	n	*t*-test		Average	s.d.	*n*	*t*-test
AM 48 hpf	Wild-type	14.8	2.8	25	*P*=0.90	Control MO	12.6	1.8	31	*P*=0.71
	glo	14.8	2.5	23		*cdh2* MO	12.8	3.0	44	
PM 48 hpf	Wild-type	11.7	2.6	26	*P*=0.01	Control MO	10.4	3.2	19	*P*=0.04
	glo	13.9	3.1	23		*cdh2* MO	8.5	2.6	31	
AM 72 hpf	Wild-type	25.6	4.2	7	*P*=0.91					
	glo	25.8	5.1	11						
PM 72 hpf	Wild-type	15	4.0	7	*P*=0.34					
	glo	16.9	4.1	11						

Whole-mount embryos were stained with Rhodamine-phalloidin and image volumes were acquired by two-photon microscopy. Image projections were made from each volume that encompassed the regions of the maculae, and hair cells were counted. AM, anterior macula; PM, posterior macula.

supporting cells and statoacoustic ganglion neurons of the developing inner ear could be influenced by cadherin adhesion molecule activities.

Zebrafish N-cadherin gene mutants (alleles of the *parachute* and *glass onion* genes; *pac/glo/ncad/cdh2*) have been identified (Lele et al., 2002; Malicki et al., 2003), but an ear phenotype was not reported. We reported that Cdh2/*cdh2* protein and message are expressed in the developing inner ear, accumulating in the developing sensory patches that give rise to the hair cells and supporting cells (Novince et al., 2003), which suggests that Cdh2 might be involved in the regulation of sensory patch formation. Here we test this hypothesis by examining the effects of *cdh2* loss-of-function through application of antisense oligonucleotide (morpholino oligonucleotides; MOs) knockdown experiments (MO-induced phenotype is referred to as morphant phenotype, in contrast to mutant phenotype) and by studying aspects of ear development in the *cdh2* mutant, *glass onion* (*glo*). These studies demonstrate similar phenotypes in the morphant and *cdh2* mutant inner ears, which demonstrate a selective role for Cdh2 in inner ear differentiation and semicircular canal morphogenesis.

Results

Cdh2 function during inner ear differentiation: loss-of-function experiments

To determine the effects of *cdh2* dysfunction on inner ear development in zebrafish, experiments were performed using translation-blocking *cdh2* MO injections in wild-type fish and the *glo* null mutation in the *cdh2* gene. The *cdh2* MO (Lele et al., 2002) and *glo* mutation have been described previously (Jiang et al., 1996; Malicki et al., 1996; Lele et al., 2002; Malicki et al., 2003). Cadherin-2-knockout mice show developmental delay due to cardiovascular defects affecting nutrient and gas exchange (Radice et al., 1997), which can be compensated for by expressing N-cadherin in the myocardium (Luo et al., 2001). In general, zebrafish embryos lacking cardiovascular function do not exhibit a developmental delay because the fish embryo is sufficiently small that gas exchange can occur through its skin. Previous studies showed that *cdh2* mutant embryos do not have delayed eye development (Jiang et al., 1996; Malicki et al., 1996; Lele et al., 2002; Malicki et al., 2003). Also, posterior lateral line nerve length (a good indicator of developmental stage), head size and body length were not affected in *glo* mutants and *cdh2* morphants, despite defects in lateral line nerve pathfinding (Kerstetter et al., 2004). We conclude that *cdh2* loss-of-function does not produce a general developmental delay, and no evidence was detected for delayed developmental timing of major inner ear developmental events (otic placode condensation, otic vesicle formation, sensory patch differentiation).

We examined the effect of *cdh2* MO on protein expression in the inner ear tissue itself (Fig. 1). Compared with control MO, injection of translation-blocking *cdh2* MO into 1-4 cell embryos resulted in a significant reduction of Cdh2 protein expression in the inner ear (Fig. 1A,B). However, otic vesicle structures form relatively normally in *cdh2* MO-injected and *glo* embryos, showing that disrupting Cdh2 expression did not block otic placode induction, condensation or vesicle cavitation. Comparison of β-catenin expression and distribution in normal and *cdh2* MO-injected (Fig. 1C,D) and *glo* mutant (data not shown) embryos showed similar levels and patterns, indicating that other cadherins expressed in the otic vesicle compensate for the loss of Cdh2 adhesion molecules. In some Cdh2 morphants, otolith number was affected, and otoliths were reduced in size (Table 2), which suggests that secretion of otolith material, differentiation of otic epithelium or morphogenesis was disrupted.

Our previous studies showed that cadherin-2 expression is first seen concomitantly with the formation of sensory patches during inner ear development (Novince et al., 2003), suggesting that Cdh2 may help to regulate the organization of sensory patches or differentiation of hair cells and supporting cells. The effect of *cdh2* MO and *glo* mutation on differentiation of sensory patches was examined by double labeling 2-day-post-fertilization (dpf) embryos with an acetylated tubulin antibody to identify the hair cell kinocilia and Rhodamine-conjugated phalloidin, which in turn identifies hair cell stereocilia. Sensory patches were disorganized in both *cdh2* MO-injected (Fig. 1E,F, Fig. 5B) and *glo* mutant embryos (data not shown). There was also a reduction in detectable kinocilia in disorganized anterior and posterior maculae of *cdh2* MO-injected embryos and in cristae (Fig. 1E,F). Those kinocilia that remained in the ears of *cdh2* MO-injected embryos were short or irregularly shaped. The length of the kinocilia and defects in *cdh2* MO-injected ears are more evident in larger volumes in volume projections of additional planes from the same image stacks that were used to produce Fig. 1E and F (see insets in these panels). These volume projections can be viewed as rotating, three-dimensional rendered volumes in Movies 1 and 2 (see supplementary material). There was also reduced tubulin staining within the

hair cells in *cdh2* MO-injected (Fig. 1F) and *glo* mutant embryos (not shown), indicating that Cdh2 expression affects assembly of the cytoplasmic microtubule network.

Extensive quantitative analysis of the anterior and posteromedial macula showed that there was no statistically significant difference in the average number of hair cells per sensory patch identified by labeling actin fibers with phalloidin in *cdh2* MO-injected and *glo* mutant embryos compared with control embryos (either control MO-injected or wild type embryos from *glo* heterozygote crosses; Table 1). Two-photon microscopy was used to image the entire developing otic vesicle. Each otic vesicle image stack was examined by rotation of the three-dimensional rendered volume to ensure that hair cells were identified unambiguously (data not shown).

Cellular junctions in the anterior macula were maintained in *glo* mutant ears

To determine whether cell-cell adhesion or hair cell morphology were disrupted, we performed a transmission electron microscopy study of the inner ear in control, *cdh2* morphants (Fig. 2) and in *glo* mutants (data not shown). The stereocilia bundles on hair cells in the anterior macula in *cdh2* morphants (Fig. 2D,E) and *glo* mutants (not shown) were normally structured, compared with the maculae of control fish (Fig. 2A,B). Adhesion between otic epithelial cells showed occasional gaps in *cdh2* morphants and *glo* mutants, but epithelial cells generally showed closely apposed plasma membranes and well-developed adherens junction structures (compare Fig. 2C with 2F). These data indicate that adherens junctions are morphologically normal despite loss of Cdh2 expression; and the hair cell bundle of kinocilia and stereocilia are well organized despite effects on kinocilia in *glo* mutants and Cdh2 morphants.

cdh2 loss-of-function does not prevent otic induction

To examine how *cdh2* loss-of-function affects the expression of early genes in the inner ear that serve as markers of otic epithelial specification and patterning, we performed an in situ hybridization study. Claudin a (Cldna) is a tight-junction protein that is specifically expressed in the junctional complexes of the inner ear epithelial cells that line the otic vesicle (Kollmar et al., 2001). By 24 hours post fertilization (hpf), *cldna* mRNA is seen on the luminal side of the inner ear epithelial cells (Fig. 3A). In the *cdh2* morphants (not shown) and *glo* mutants (Fig. 3B), *cldna* expression was as extensive as the controls, although the morphant and mutant ears themselves were sometimes more compact.

The expression of the transcription factor gne *dlx3b* was also examined. Zebrafish *dlx3b* is expressed in the olfactory placode, visceral arches and otic vesicles by 24 hpf (Fig. 3C) (Ekker et al., 1992; Liu et al., 2003). A reduction in Cdh2 function resulted in a more pronounced *dlx3b* signal in the ear at 24 hpf (Fig. 3D), similar to the results of MO treatment on *cldna* expression. This appearance, too, is probably the result of a more compact epithelium in the inner ear of morphants and mutants.

Pax2a is a homeodomain-containing transcription factor, and *pax2a* message (Fig. 3E,F) was detected in the optic stalk, midbrain-hindbrain boundary, and was expressed weakly in the hindbrain, and in the otic vesicles at 24 hpf (Fig. 3E) (Krauss et al., 1991; Liu et al., 2003; Hans et al., 2004). Again, the

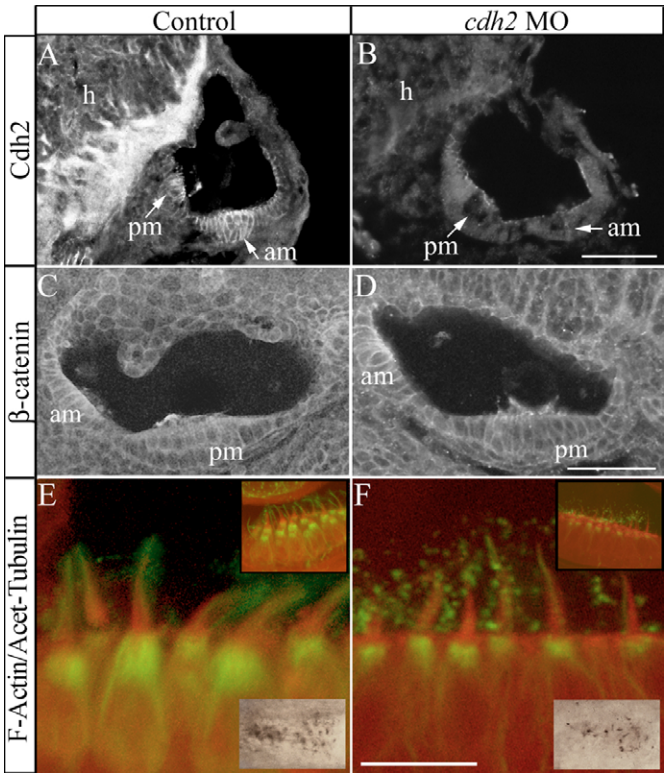

Fig. 1. Loss of Cdh2 affects kinocilia and cellular microtubule networks. Panels A and B are transverse sections tilted to include both the anterior and posterior maculae in the same view of 48 hpf embryos labeled with anti-Cdh2 antibody. In control embryos the anterior (am) and posterior maculae (pm), are strongly labeled by Cdh2 (A). Cdh2 immunolabeling of sensory patches in *cdh2* MO-injected embryos is absent (B). Panels C and D are image volumes acquired by two-photon microscopy of 48 hour post-fertilization whole-mount zebrafish stained using anti-β-catenin. Projections are 6 μm optical sections of a lateral view of the regions containing the anterior and posterior maculae (am and pm) in a control (C) and in a *cdh2* MO-injected embryo. Rostral is left, dorsal is up and ventral is down. Panels E, F are projections of two optical sections through the anterior maculae of 120 hpf embryos labeled with anti-acetylated-tubulin (shown in green) to visualize kinocilia and Texas-Red-conjugated phalloidin (shown in white) to visualize hair cell sterociliary bundles. Well-formed kinocilia are present in hair cell bundles in control embryos (E), but reduced in *cdh2* MO-injected embryos. This is especially evident in the insets in panels E and F, showing images of acetylated-tubulin-labeled posterior maculae from 48 hpf embryos using DAB/peroxidase detection (bottom insets), and a larger rendered volume from the image stack used to make panels E and F (upper inset; this volume can be viewed as rotating, three-dimensional rendered volumes in Movies 1 and 2, see supplementary material). Ciliary bundles in control embryos each correspond to a kinocilium. In *cdh2* MO-injected embryos, hair cell bundles are associated with short kinocilia, or kinocilia are absent. Abbreviations: h, hindbrain. Bars: A-D, 50 μm; E-F, 10 μm.

morphants (not shown) and *glo* mutants (Fig. 3F) demonstrated a more concentrated or contracted labeling pattern in the otic vesicles.

In contrast to these relatively normal expression patterns, differences were seen in comparisons of the expression domain of *fgf8* (encoding fibroblast growth factor 8). Early zebrafish *fgf8* expression in the hindbrain participates in otic placode

Table 2. Loss of Cdh2 does not affect inner ear volume

Ear morphology		Small ears	Small otoliths	One otolith	Three or fused otoliths	*n*
50-52 hpf	Control	6.7%	0%	0%	6.7%	30
	cdh2 MO	10.5%	2.1%	5.6%	25.9%	143
70-79 hpf	Control	0%	0%	0%	9.1%	11
	cdh2 MO	2.1%	2.1%	2.1%	25.5%	47

Inner ear volume	Volume (μm^3)	s.d. (μm^3)	*n*	*t*-test
Wild-type	171,034	62,338	30	*P*=0.50
glo	159,725	70,561	31	
Control MO	152,227	45,158	5	*P*=0.95
cdh2 MO	150,390	79,630	15	

Slight size differences were seen between controls and Cdh2-deficient embryos when embryos were classified by external ear morphology. No difference was seen when whole-mount embryos were stained with rhodamine-phalloidin and image volumes were acquired by two-photon microscopy and then used to determine the fluid volume of the inner ear.

induction, and *fgf8* is expressed later in the otic vesicle (Liu et al., 2003). By 24 hpf, *fgf8* is expressed in the dorsal diencephalon, facial ectoderm, optic stalk and otic vesicles; *fgf8* expression was seen in the ventroanterior quadrant at this stage, and the *cdh2* morphants showed a similar expression pattern at this time (Fig. 3H). However, by 48 hpf, the expression domain of *fgf8* was shifted to the ventral side of the ear in control embryos (Fig. 3I), while in many morphants, the expression remained on the anterior side of the ear (Fig. 3J), suggesting either that the expression domain has shifted or the orientation of the ear has been affected by the loss of Cdh2.

Statoacoustic ganglion formation was inhibited by cdh2 loss-of-function

Differentiation of statoacoustic ganglion neurons was examined in *cdh2* MO-injected and *glo* mutant embryos. Statoacoustic ganglion cells in 36-38 hpf embryos were stained using antibody markers for neuronal differentiation that label the statoacoustic ganglia in zebrafish, anti-Hu antibodies (that recognize neuronal protein HuC/Hu; data not shown) and monoclonal antibody zn-5 (that recognizes neurolin/DMGRASP; Fig. 4). The circumference of the statoacoustic ganglion was measured from camera lucida drawings of labeled embryos. The average circumference was significantly reduced due to *cdh2* loss-of-function (Fig. 4). Cdh2 therefore contributes to the correct morphogenesis of the statoacoustic ganglion.

Inner ear morphogenesis defects are due to *cdh2* loss-of-function

Three-dimensional image volumes of phalloidin-labeled embryos showed that *cdh2* MO-injected and *glo* mutant embryos did not develop normal semicircular canals. To examine the effect of *cdh2* dysfunction on semicircular canal formation, advanced image analysis was performed on two-photon microscope image stacks. In phalloidin-stained ears, the brightly labeled apical membranes of epithelial cells that line the otic vesicle delimit the fluid space, which is not labeled and appears very black. Segmentation analysis was used to identify the fluid volume (Fig. 5A-J). Rotation of the segmented fluid volume allowed us to examine the shape of the

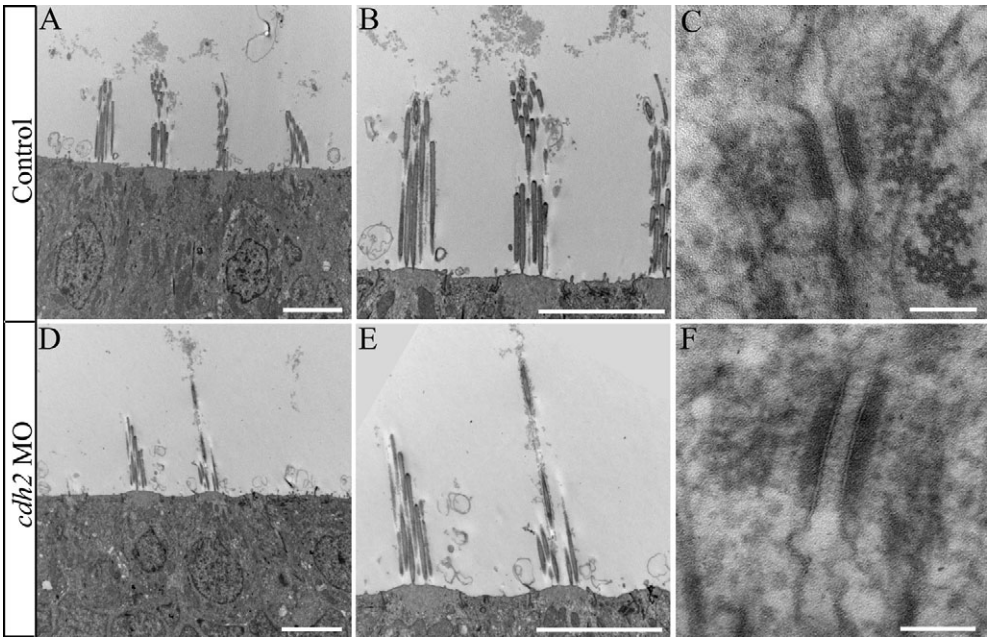

Fig. 2. Cellular junctions are maintained in *cdh2* morphant. Transmission electron micrographs of anterior macula from 5 dpf ears from control (A-C) and *cdh2* morphants (D-F) embryos show little or no change in cellular morphology (see text for details). Abbreviations: hb, hair cell bundles; hc, hair cell; sc, supporting cell. Bars: A, B, D, E, 5 μm; C,F, 100 nm.

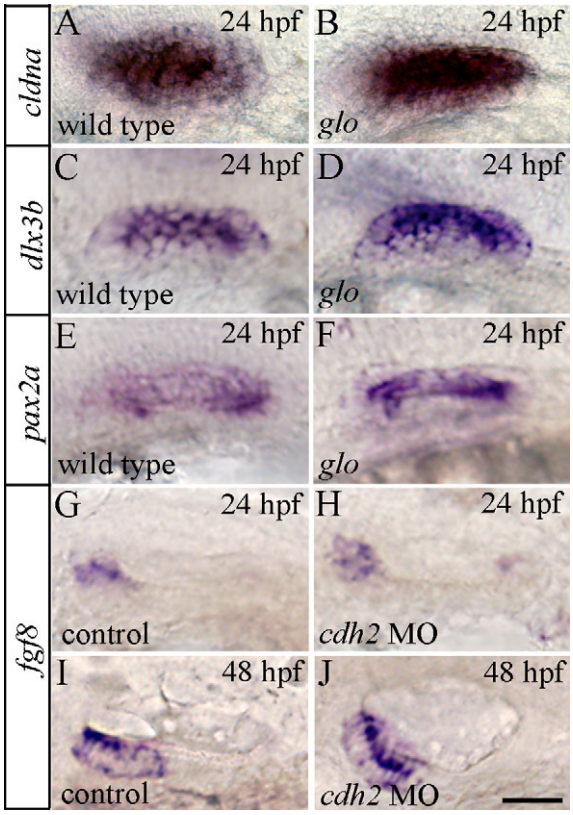

Fig. 3. Loss-of-function of Cdh2 does not inhibit otic induction. Whole-mount in situ hybridizations with a *cldna* (A,B), *dlx3b* (C,D), *pax2a* (E,F), and *fgf8* (G-J) probes, early markers of otic induction, in wild-type control embryos (A,C,E), *glo* mutant embryos (B,D,F), control MO-injected embryos (G,I) and *cdh2* MO-injected embryos (H,J). Panels are lateral views with anterior to the left and dorsal side up. A-H are 24 hpf embryos and I-J are 48 hpf embryos. Bar, 50 μm.

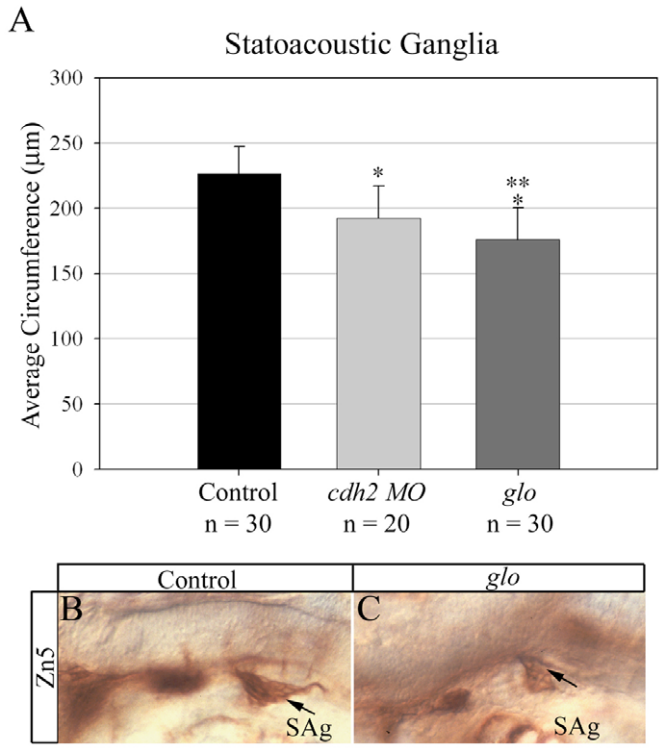

Fig. 4. Statoacoustic ganglia are reduced in size in *cdh2* mutants and knockdowns. Statoacoustic ganglia (SAg) were labeled with zn-5 in 36 hpf control (B), *glo* (C) and *cdh2* MO-injected embryos. Circumferences of zn-5 labeled SAgs were measured (A). The average circumference of control SAgs (226.8 μm) was greater than that of *cdh2* MO-injected embryos (192.3 μm, $P<0.001$) and of *glo* mutant embryos (176.2 μm, $P<0.001$). Average SAg circumference was smaller in the *glo* null mutant than in *cdh2* MO-injected knockdowns ($P<0.05$).

fluid space to visualize semicircular canals of the developing inner ear (Fig. 5K-T).

Segmented fluid volumes from phalloidin-labeled inner ears were also used to quantify the volume of the otic vesicle fluid space. Fluid volume measured using segmentation analysis of two-photon microscope image volumes of phalloidin-labeled embryos showed that the inner ear fluid volume of *cdh2* MO-injected and *glo* mutant embryos was not statistically different from that of control MO-injected and wild-type embryos (Table 2). Observation by transmitted light microscopy showed that otic vesicles of *cdh2* MO-injected and *glo* mutant embryos were somewhat smaller (Table 2). Since fluid volumes were unchanged by *cdh2* loss-of-function, the change in otic vesicle size could be the result of a change in the overall inner ear architecture due to a failure to form normal semicircular canals. Size change was not due to altered rates of proliferation or apoptosis. Rates of proliferation were measured by counting numbers of histone H3-positive cells apposing the otic vesicle lumen at 52 hpf: control embryos (23.6±5.8, $n=5$) and Cdh2 morphant embryos (21.0±7.7, $n=12$) were not statistically different ($P=0.46$). Apoptosis was nearly undetectable in otic epithelial cells of control embryos and *cdh2* MO-injected embryos at both 48 and 52 hpf (using acridine orange staining; data not shown).

Analysis of phalloidin-labeled embryonic inner ear volumes demonstrated that Cdh2 was required for extension of cellular bridges during semicircular canal morphogenesis. At around 42 hpf, the epithelium begins to develop protrusions that grow out and extend into the lumen. Pairs of opposing projections at the anterior and posterior ends of the vesicle extend, meet and then fuse to form the hub of tissue that forms the pillars of the semicircular canals (Waterman and Bell, 1984; Haddon and Lewis, 1996). In control embryos (either control MO-injected or wild-type embryos from *glo* heterozygote crosses), at least one cellular bridge was connected across the otic vesicle in most individuals at 48 hpf, and both cellular bridges were connected in the remaining cases (Fig. 6). In *cdh2* MO-injected and *glo* mutant embryos, the phenotype ranged from one connected cellular bridge to the absence of any cellular extensions (Fig. 6), and the morphology distributions in wild-type and *glo* mutant embryos were statistically different (Fig. 6).

Discussion

Our previous studies showed that Cdh2/*cdh2* is expressed as soon as sensory patches form during inner ear development, and expression increases with patch size (Novince et al., 2003), suggesting that Cdh2 may contribute to the organization of sensory patches or differentiation of hair cells and supporting

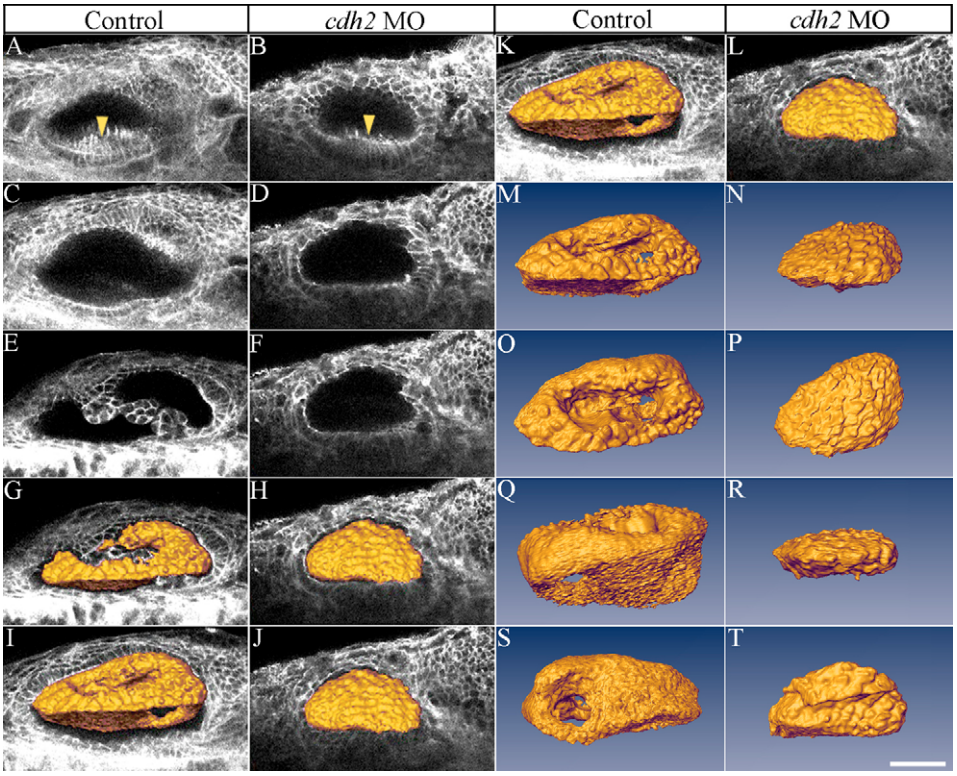

Fig. 5. Surface renderings of segmented inner ear volumes facilitate assessment of differences in morphology and allow unbiased measurement of inner ear volume. Panels A-F are optical sections acquired by two-photon microscopy of 48 hour post-fertilization zebrafish stained using Texas-Red-conjugated phalloidin. Lateral is up and rostral is to the right. Sections of the most ventral region of the ear (A,B) show that the posterior macula of the *cdh2* MO-injected embryo (arrow in B) contains shorter stereociliary bundles compared with those of the control (arrow in A). Sections taken from more dorsal regions of the ears (E,F) show semicircular canals in the control embryo (E) which are absent in the *cdh2* MO-injected embryo (F). To show the relationship of the optical sections to the surface rendered volumes, the optical sections from panels E and F are shown cutting through surface renderings of the volume of the inner ear in control (G) and in *cdh2* MO-injected embryos (H). In the bottom panels, the entire volume of the inner ears are shown in control (I) and in *cdh2* MO-injected embryos (J) relative to the most ventral optical sections. Panels K and L are shown to provide orientation of the rendered volume relative to the optical sections. Shown directly below are the surface renderings of inner ear volumes from a 48 hpf control (M,O,Q,S) and *cdh2* MO-injected (N,P,R,T) embryos, first in the same orientations as in K and L, then rotated. Image volumes were segmented and volume measurements were generated using Amira software (Table 2). Semicircular canals pass through the control volume (M,O,Q,S), but are entirely absent from the *cdh2* MO-injected embryo volume (N,P,R,T). In M-P, lateral is up, rostral is right and the view is of the dorsal side of the volume. In Q and R, dorsal is up, caudal is right and the view is of the lateral side. In S and T, dorsal is up caudal is right and the view is of the medial side. Bar, 50 μm.

cells. We tested these ideas by using morpholino knockdown technology and by examining *cdh2* null mutant (*glo*) embryos. Zebrafish inner ear morphogenesis has been described (Haddon and Lewis, 1996; Bever and Fekete, 2002; Whitfield et al., 2002). However, complex molecular and cellular interactions that guide development from otic placode induction through otic vesicle lumen cavitation, differentiation of specific cell types (including statoacoustic ganglion neurons) and semicircular canal morphogenesis are largely unknown (Barald and Kelley, 2004).

Disrupting Cdh2 expression did not prevent the earliest stages of otogenesis, otic placode induction and vesicle cavitation. Increased adhesion between ectodermal cells during placode condensation may well be mediated by other cadherins, but our findings indicated that Cdh2 is not required during this process. Normal numbers of hair cells were present as detected using phalloidin to stain actin-containing hair cell bundles. However, using acetylated tubulin antibodies to detect the kinocilium, it was apparent that *cdh2* loss-of-function resulted in fewer detectable kinocilia, and those present in these ears were short and irregularly shaped. Very little precedent exists for a connection between cadherin adhesion and epithelial cilia formation. However, there have been reports that polycystic kidney disease gene products are associated with the adherens junction and primary cilium (Eley et al., 2004). Also, cadherin adhesion activates Rac1 and Cdc42 GTPase signaling pathways (Kim et al., 2000; Nakagawa et al., 2001; Noren et al., 2001), which in turn activate the atypical protein kinase C (aPKC)-Par complex (reviewed in Suzuki and Ohno, 2006). This signaling cassette was shown to regulate primary cilium assembly in epithelial cells (Fan et al., 2004). It is interesting that *heart and soul* mutant embryos, which have a defect in the atypical protein kinase C gene, also have defective semicircular canal formation (S.B.-C. and J.A.M., unpublished). Additional investigation will be required to determine whether adherens junction signaling regulates cilia assembly, particularly the elaboration of the kinocilium of inner ear hair cells.

The otic vesicle is partitioned by the expression of various developmental signaling molecules to pattern domains of the developing inner ear. We examined expression patterns of a set of these molecules in normal embryos and Cdh2-deficient embryos. Areas of expression domains were expanded for some markers and others were reduced, suggesting a mild effect on patterning. For example, altered expression of *fgf8* in *cdh2* morphants may show a shifted patterning within the otic vesicle. However, expression domains were not entirely eliminated, showing that specification of inner ear epithelium within the otic vesicle occurred in the absence of Cdh2. It is possible that changes in vesicle morphogenesis or adhesion between cells within a domain could cause the collapse or rotation of expression domains into another area of the vesicle.

We also found that Cdh2 participates in statoacoustic ganglion development, suggesting that cranial nerve connection

for the inner ear was functionally impaired. Further investigation will be required to determine whether neurogenesis, gliogenesis or connectivity have been affected and at what stage. There may be other redundant adhesion molecules (perhaps other cadherins) that control statoacoustic ganglion development (Novince et al., 2003), which permit limited statoacoustic ganglion formation. Double knockdown experiments are required to determine whether more than one cadherin collaborates in statoacoustic ganglion formation. We did not detect an increase in cell death caused by *cdh2* loss-of-function (data not shown), which supports the conclusion that statoacoustic ganglion differentiation and/or delamination were affected rather than survival of the ganglion neuronal precursors after differentiation. Together, these findings suggest that Cdh2 affects differentiation, not only of statoacoustic ganglion neurons but of sensory hair cells. It remains to be determined whether this effect is mediated through a common precursor or through reciprocal interactions between hair cells and neurons in the formation or maintenance of connections (Barald and Kelley, 2004). This conclusion is also supported by our findings of reduced kinocilia formation and altered hair cell morphology.

It is important to note that there are considerable effects on hindbrain development that occur as a consequence of Cdh2 deficiency (Jiang et al., 1996; Lele et al., 2002), and signals emanating from the hindbrain profoundly affect inner ear development (Barald and Kelley, 2004 and reviews cited therein) (Whitfield et al., 2002; Liu et al., 2003; Hans et al., 2004). Therefore, the effects of Cdh2 knockdown and *glo* null mutation could indirectly affect ear development via hindbrain signals. However, Cdh2 is expressed in the otic vesicle itself, particularly in the forming sensory patches. Therefore, it is reasonable to think that Cdh2 expression in the inner ear participates in cellular activities such as morphogenetic movements during the formation of the otic structures, but effects of Cdh2 expression in the ear and hindbrain should be distinguished.

We detected a modest effect of *cdh2* loss-of-function on otic vesicle length. Perhaps the shape changes caused by semicircular canal morphogenesis make the otic vesicle longer. Loss of normal Cdh2 function does not result in widespread dysadhesion and delamination of cells within the otic vesicle epithelium, probably because there are other cadherins expressed within the developing otic vesicle (Novince et al., 2003) that compensate for *cdh2* loss-of-function.

The most significant finding of this study is that Cdh2 dysfunction interfered with the ability of otic vesicle epithelial cells to extend cellular processes and to connect these cellular processes to a similar process from the opposite surface of the otic vesicle, forming the cellular bridges that produce the fluid-filled semicircular canals. It is interesting to note that the cells in the wall of the otic vesicle adjacent to the epithelial protrusion have reduced Cdh2 protein expression (Fig. 1A). High expression levels of Cdh2 in the sensory patches relative to neighboring otic epithelial cells may induce folding or buckling of the epithelium. This may indirectly affect folding due to differences in adhesion forces. Cdh2 knockdown often prevented the sorting of hair cells and supporting cells into two distinct layers (for example, see Fig. 1D).

Other cellular mechanisms than adhesion may control sensory epithelium cell shape and morphogenetic movements. Morphogenetic cell movements that occur during semicircular canal formation are analogous to tubulovesicular developmental processes such as those modeled by MDCK cells (O'Brien et al., 2002; Zegers et al., 2003). Cadherin adhesion was identified previously as a key regulator of both cystogenesis and tubulogenesis in epithelial cells (Bazzoni et al., 1999; Troxell et al., 2001; Chihara et al., 2003). Additional factors that regulate adhesion and polarity in epithelial cells are also critical for MDCK cyst and tubule formation, for example, Rho family GTPase and APC (Pollack et al., 1997; O'Brien et al., 2001; Yu et al., 2005). We detected changes in the microtubule network that result from *cdh2* loss-of-function. APC-mediated cell movements are driven by its association with the microtubule cytoskeleton (Nathke et al., 1996; Mimori-Kiyosue et al., 2000; Mogensen et al., 2002; Watanabe et al., 2004). It is useful to note that previous studies showed specific effects of cadherin-mediated cell-cell adhesion on microtubule cytoskeleton assembly and how connection of cadherin molecules to microtubule motors affects junction assembly (Chausovsky et al., 2000; Ligon

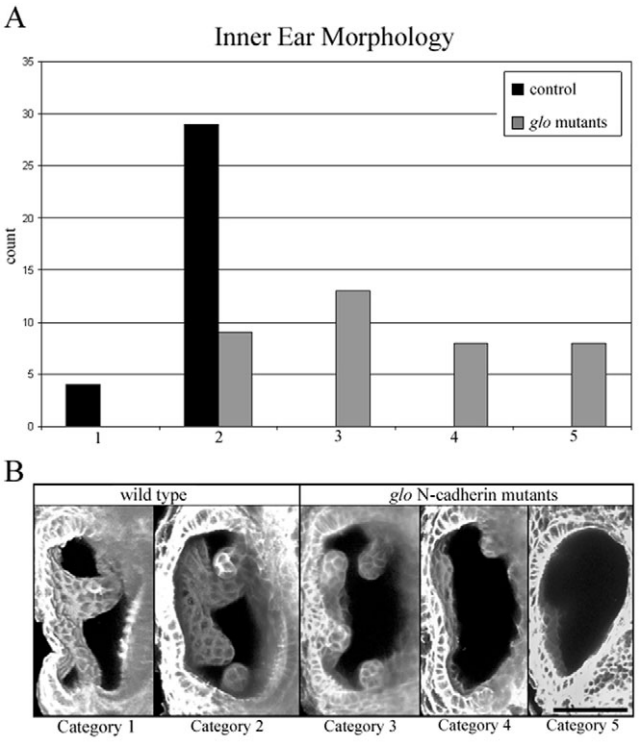

Fig. 6. Projection images of the inner ear reveal morphological distinctions between control and *glo* mutant embryos. Whole-mount embryos were stained with Texas-Red-conjugated phalloidin and image volumes were acquired by two-photon microscopy. Image projections were made from each volume that encompassed the region of the lateral, rostral and caudal epithelial projections into the otic vesicle. Each ear was classified by extent of epithelial projection formation and fusion (B, see Materials and methods for description of classification scheme). Control embryos (n=33) all were either category 1 or 2, with fully formed projections and fusion of at least the rostral and lateral epithelial pillars. *glo* mutant embryos (n=38) were spread across categories 2-5, with most lacking any fusion of epithelial pillars (A). Wild-type and *glo* mutant morphology were statistically different ($P=8.6\times10^{-9}$, df=4, Chi Square=43.39). Bar, 50 μm.

et al., 2001; Chen et al., 2003). Perhaps Cdh2 regulates microtubule-based and cytoskeleton-mediated epithelial cell shape changes via APC or an analogous mechanism. It would be of interest to examine the effects of these signaling pathways during inner ear formation.

Materials and Methods

Zebrafish

Zebrafish (*Danio rerio*) were raised and kept under standard laboratory conditions (Westerfield, 2000) in accordance with Indiana University, University of Akron and University of Michigan policies on animal care and use. The *glass onion* (*glo*) mutant embryos were obtained from the Zebrafish International Resource Center at the University of Oregon (Eugene, OR). For some experiments, 0.2 mM phenylthiourea (PTU) was added to embryo medium to prevent melanization.

Morpholino injection

Morpholino oligonucleotides [*cdh2* MO1 and MO2 (Lele et al., 2002); control: Gene Tools, Covalis, OR) were microinjected into the yolk of one- to four-cell stage embryos (Ekker, 2000). Injected embryos were allowed to develop at 28.5°C until the appropriate developmental stage.

Immunolabeling

Embryos were fixed overnight in 4% paraformaldehyde in phosphate buffered saline at 4°C. Affinity purified Cdh2 polyclonal antibody, generated against the entire EC1 domain of zebrafish Cdh2, was used as described previously (Liu et al., 2001). Anti-acetylated tubulin antibody (Sigma, St Louis, MO) used at 1:3000, and anti-β-catenin antibody (Transduction Labs) used at 1:200 were followed by Alexafluor 488-conjugated anti-mouse (Molecular Probes), TRITC-conjugated anti-mouse or TRITC-conjugated anti-rabbit (Jackson ImmunoResearch) at 1:50 dilutions. For insets in Fig. 1E and F, 48 hpf embryos were labeled using acetylated tubulin antibodies (as above), and then these embryos were processed using biotinylated anti-mouse IgG (Vector Labs, Burlingame, CA) and detected with avidin-conjugated horseradish peroxidase, visualized with DAB (Vector Labs). The zn-5 antibody (Zebrafish Resource Center, Eugene, OR) was used at 1:2000 dilution, followed by biotinylated anti-mouse IgG (Vector Labs, Burlingame, CA) and detected with avidin-conjugated horseradish peroxidase, visualized with DAB (Vector Labs). Texas-Red-conjugated phalloidin (Molecular Probes, Carlsbad CA) was used at 1:200. Tissue sections and DAB-labeled whole mounts were viewed with epifluorescence or Nomarski lenses with an Olympus microscope system (BX 51) (Melville, NY). Two-photon microscope image volumes were acquired using a Zeiss LSM-510 Meta Confocal microscope System (Göttingen Germany) equipped with a tunable Titanium-Sapphire laser.

Segmentation of inner ear volume

Measurements of inner ear volume using segmented images allow comparison of inner ear size that is unbiased by shape changes that commonly correspond with changes in morphology. Two day post-fertilization whole-mount embryos were labeled with Texas-Red–phalloidin and 3D image stacks were acquired using two-photon microscopy. Phalloidin labeling resulted in brightly stained cell membranes that were sharply demarcated from the black space of the inner ear volume. Inner ear volumes were then segmented with a 3D region-growing algorithm using Amira (Mercury Computer Systems, San Diego, CA). The segmented volumes were then used to calculate the volume of the inner ear by multiplying voxel volume by the number of voxels encompassed by the segmented volume. For visualization, a surface was created from the corresponding segmented volume and composited with the rendered 3D volume.

Hair cell counting

Two day post-fertilization whole-mount embryos were labeled with Texas-Red–phalloidin and 3D image stacks were acquired using two-photon microscopy. Projection images of control and *cdh2* MO-injected embryos and *glo* embryos were rendered using Voxx (Clendenon et al., 2002). Rendered volumes were rotated and viewed from various angles with and without overlying planes removed to unambiguously identify and count all hair cell bundles. This advanced visualization technique was especially important in counting hair cells in the Cdh2-deficient embryos, whose hair cells tended to be shorter and less easily discerned by conventional methods.

Classification of semicircular canal formation

Two day post-fertilization whole-mount embryos were labeled with Texas-Red–phalloidin and 3D image stacks were acquired using two-photon microscopy. Projection images of the planes containing epithelial bulges and projections of control and *glo* embryos were rendered using Voxx (Clendenon et al., 2002), then examined and classified into categories by the extent of semicircular canal formation. In category 1 embryos, both rostral and caudal projections have contacted and fused with the lateral projection. Category 2 embryos have distinct lateral, rostral and caudal projections with contact and fusion between the rostral and lateral protrusions only. Category 3 embryos have distinct lateral, rostral and caudal projections, but no fusion. Category 4 has some rounded bulges, but they do not project into the otic cavity. Category 5 embryos lack any epithelial bulges or projections into the otic cavity.

In situ hybridization

Whole-mount in situ hybridization was performed as described (Barthel and Raymond, 1990; Liu et al., 1999; Doudou et al., 2004). Digoxigenin-labeled riboprobes for *claudin a* (Kollmar et al., 2001), *pax2a* (Krauss et al., 1991), *fgf8* (Reifers et al., 1998), *dlx3b* (Ekker et al., 1992) were synthesized from cDNA as run-off transcripts from linearized templates by using the Genius System DIG RNA Labeling Kit. Probes were detected using an alkaline-phosphatase-conjugated antibody and visualized with 4-nitroblue tetrazolium/5-bromo-4-chloro-3-indolyl phosphate (NBT/BCIP; Roche Molecular Biochemicals, Indianapolis, IN). Embryos were analyzed using an Olympus BX-51 microscope in the Microscopy and Image Analysis Laboratory at the University of Michigan.

Transmission electron microscopy

Whole-mount 5 dpf and 3 dpf embryos were anaesthetized with 0.02% 3-aminobenzoic acid ethyl ester, cut through the head behind the ears, and fixed in 2.5% glutaraldehyde in 0.1 M Sorensen's buffer (Electron Microscopy Sciences, Hatfield, PA) overnight at 4°C. Specimens were post-fixed in 1% OsO_4 in 0.1 M Sorensen's buffer for 1 hour, followed by staining with 5% uranyl acetate in H_2O for 1 hour and then dehydrated by serial steps in ethanol, embedded in Embed 812 (Electron Microscopy Sciences) or Epon and polymerized at 60°C for 24 hours. Ultrathin sections (70-90 nm) were cut then stained with uranyl acetate or alternatively stained with lead citrate and uranyl acetate. Sections were viewed on a Tecnai BioTwin (FEI, Hillsboro, OR) and digital images were acquired with an AMT CCD camera (Advanced Microscopy Techniques, Canvers, MA) in the Indiana University Electron Microscopy Center, or analyzed with a Phillips CM-100 electron microscope (Philips Electron Optics, Eindhoven, The Netherlands) in the Microscopy and Image Analysis Laboratory at the University of Michigan.

We thank Cunming Duan, Rob Cornell, Michael Brand, Jeremy Wegner, Dong Liu and Monte Westerfield for probes and plasmids. We thank Jaqueline McMillan and Karen Wu, University of Michigan for excellent technical assistance, and Christopher Cooke and Maria Xiang for fish care (University of Michigan). Two-photon images were acquired at the Indiana Center for Biological Microscopy, which is partially funded by a grant (Indiana Genomics Initiative) from the Lilly Endowment to the Indiana University School of Medicine. We acknowledge the IU School of Medicine Electron Microscopy Center and the NIH grant S10-RR17754, which supported the purchase of the transmission electron microscope. In addition, transmission electron micrographs were acquired at the University of Michigan Microscopy Image Analysis Laboratory, and we thank Dorothy Sorenson for technical assistance. We thank the Zebrafish International Resource Center for providing *glo* carrier embryos. This work was supported by a grant from the NIH to J.A.M., K.F.B. and Q.L. (RO1 DC006436) and by grants from the DRF and the NIH to K.F.B. (NIH DC05939 and DC04184) as well as NIH training grant support to Y.-c.S. (T32 DC00011 University of Michigan).

References

Babb, S. G. and Marrs, J. A. (2004). E-cadherin regulates cell movements and tissue formation in early zebrafish embryos. *Dev. Dyn.* **230**, 263-277.

Babb, S. G., Kotradi, S. M., Shah, B., Chiappini-Williamson, C., Bell, L. N., Schmeiser, G., Chen, E., Liu, Q. and Marrs, J. A. (2005). Zebrafish R-cadherin (Cdh4) controls visual system development and differentiation. *Dev. Dyn.* **233**, 930-945.

Barald, K. F. and Kelley, M. W. (2004). From placode to polarization: new tunes in inner ear development. *Development* **131**, 4119-4130.

Barthel, L. K. and Raymond, P. A. (1990). Improved method for obtaining 3-microns cryosections for immunocytochemistry. *J. Histochem. Cytochem.* **38**, 1383-1388.

Bazzoni, G., Dejana, E. and Lampugnani, M. G. (1999). Endothelial adhesion molecules in the development of the vascular tree: the garden of forking paths. *Curr. Opin. Cell Biol.* **11**, 573-581.

Bever, M. M. and Fekete, D. M. (2002). Atlas of the developing inner ear in zebrafish. *Dev. Dyn.* **223**, 536-543.

Chausovsky, A., Bershadsky, A. D. and Borisy, G. G. (2000). Cadherin-mediated regulation of microtubule dynamics. *Nat. Cell. Biol.* **2**, 797-804.

Chen, X., Kojima, S., Borisy, G. G. and Green, K. J. (2003). p120 catenin associates with kinesin and facilitates the transport of cadherin-catenin complexes to intercellular junctions. *J. Cell Biol.* **163**, 547-557.

Chihara, T., Kato, K., Taniguchi, M., Ng, J. and Hayashi, S. (2003). Rac promotes epithelial cell rearrangement during tracheal tubulogenesis in Drosophila. *Development* **130**, 1419-1428.

Clendenon, J. L., Phillips, C. L., Sandoval, R. M., Fang, S. and Dunn, K. W. (2002). Voxx: a PC-based, near real-time volume rendering system for biological microscopy. *Am. J. Physiol. Cell Physiol.* **282**, C213-C218.

Doudou, E., Barald, K. F. and Postlethwait, J. H. (2004). Over-expression of Zic2a rescues ventralized zebrafish embryos. *Zebrafish* **1**, 239-257.

Ekker, M., Akimenko, M. A., Bremiller, R. and Westerfield, M. (1992). Regional expression of three homeobox transcripts in the inner ear of zebrafish embryos. *Neuron* **9**, 27-35.

Ekker, S. C. (2000). Morphants: a new systematic vertebrate functional genomics approach. *Yeast* **17**, 302-306.

Eley, L., Turnpenny, L., Yates, L. M., Craighead, A. S., Morgan, D., Whistler, C., Goodship, J. A. and Strachan, T. (2004). A perspective on inversin. *Cell Biol. Int.* **28**,119-124.

Ernest, S., Rauch, G. J., Haffter, P., Geisler, R., Petit, C. and Nicolson, T. (2000). Mariner is defective in myosin VIIA: a zebrafish model for human hereditary deafness. *Hum. Mol. Genet.* **9**, 2189-2196.

Fan, S., Hurd, T. W., Liu, C. J., Straight, S. W., Weimbs, T., Hurd, E. A., Domino, S. E. and Margolis, B. (2004). Polarity proteins control ciliogenesis via kinesin motor interactions. *Curr. Biol.* **14**, 1451-1461.

Gumbiner, B. M. (2005). Regulation of cadherin-mediated adhesion in morphogenesis. *Nat. Rev. Mol. Cell. Biol.* **6**, 622-634.

Haddon, C. and Lewis, J. (1996). Early ear development in the embryo of the zebrafish, Danio rerio. *J. Comp. Neurol.* **365**, 113-128.

Hans, S., Liu, D. and Westerfield, M. (2004). Pax8 and Pax2a function synergistically in otic specification, downstream of the Foxi1 and Dlx3b transcription factors. *Development* **131**, 5091-5102.

Jiang, Y. J., Brand, M., Heisenberg, C. P., Beuchle, D., Furutani-Seiki, M., Kelsh, R. N., Warga, R. M., Granato, M., Haffter, P., Hammerschmidt, M. et al. (1996). Mutations affecting neurogenesis and brain morphology in the zebrafish, Danio rerio. *Development* **123**, 205-216.

Kane, D. A., McFarland, K. N. and Warga, R. M. (2005). Mutations in half baked/E-cadherin block cell behaviors that are necessary for teleost epiboly. *Development* **132**, 1105-1116.

Kerstetter, A. E., Azodi, E., Marrs, J. A. and Liu, Q. (2004). Cadherin-2 function in the cranial ganglia and lateral line system of developing zebrafish. *Dev. Dyn.* **230**, 137-143.

Kim, S. H., Li, Z. and Sacks, D. B. (2000). E-cadherin-mediated cell-cell attachment activates Cdc42. *J. Biol. Chem.* **275**, 36999-37005.

Kollmar, R., Nakamura, S. K., Kappler, J. A. and Hudspeth, A. J. (2001). Expression and phylogeny of claudins in vertebrate primordia. *Proc. Natl. Acad. Sci. USA* **98**, 10196-10201.

Krauss, S., Johansen, T., Korzh, V. and Fjose, A. (1991). Expression of the zebrafish paired box gene pax[zf-b] during early neurogenesis. *Development* **113**, 1193-1206.

Lele, Z., Folchert, A., Concha, M., Rauch, G. J., Geisler, R., Rosa, F., Wilson, S. W., Hammerschmidt, M. and Bally-Cuif, L. (2002). parachute/n-cadherin is required for morphogenesis and maintained integrity of the zebrafish neural tube. *Development* **129**, 3281-3294.

Ligon, L. A., Karki, S., Tokito, M. and Holzbaur, E. L. (2001). Dynein binds to beta-catenin and may tether microtubules at adherens junctions. *Nat. Cell. Biol.* **3**, 913-917.

Liu, D., Chu, H., Maves, L., Yan, Y. L., Morcos, P. A., Postlethwait, J. H. and Westerfield, M. (2003). Fgf3 and Fgf8 dependent and independent transcription factors are required for otic placode specification. *Development* **130**, 2213-2224.

Liu, Q., Marrs, J. A. and Raymond, P. A. (1999). Spatial correspondence between R-cadherin expression domains and retinal ganglion cell axons in developing zebrafish. *J. Comp. Neurol.* **410**, 290-302.

Liu, Q., Babb, S. G., Novince, Z. M., Doedens, A. L., Marrs, J. and Raymond, P. A. (2001). Differential expression of cadherin-2 and cadherin-4 in the developing and adult zebrafish visual system. *Vis. Neurosci.* **18**, 923-933.

Luo, Y., Ferreira-Cornwell, M., Baldwin, H., Kostetskii, I., Lenox, J., Lieberman, M. and Radice, G. (2001). Rescuing the N-cadherin knockout by cardiac-specific expression of N- or E-cadherin. *Development* **128**, 459-469.

Malicki, J., Neuhauss, S. C., Schier, A. F., Solnica-Krezel, L., Stemple, D. L., Stainier, D. Y., Abdelilah, S., Zwartkruis, F., Rangini, Z. and Driever, W. (1996). Mutations affecting development of the zebrafish retina. *Development* **123**, 263-273.

Malicki, J., Jo, H. and Pujic, Z. (2003). Zebrafish N-cadherin, encoded by the glass onion locus, plays an essential role in retinal patterning. *Dev. Biol.* **259**, 95-108.

Mimori-Kiyosue, Y., Shiina, N. and Tsukita, S. (2000). Adenomatous polyposis coli (APC) protein moves along microtubules and concentrates at their growing ends in epithelial cells. *J. Cell Biol.* **148**, 505-518.

Mogensen, M. M., Tucker, J. B., Mackie, J. B., Prescott, A. R. and Nathke, I. S. (2002). The adenomatous polyposis coli protein unambiguously localizes to microtubule plus ends and is involved in establishing parallel arrays of microtubule bundles in highly polarized epithelial cells. *J. Cell Biol.* **157**, 1041-1048.

Montero, J. A., Carvalho, L., Wilsch-Brauninger, M., Kilian, B., Mustafa, C. and Heisenberg, C. P. (2005). Shield formation at the onset of zebrafish gastrulation. *Development* **132**, 1187-1198.

Nakagawa, M., Fukata, M., Yamaga, M., Itoh, N. and Kaibuchi, K. (2001). Recruitment and activation of Rac1 by the formation of E-cadherin-mediated cell-cell adhesion sites. *J. Cell Sci.* **114**, 1829-1838.

Nathke, I. S., Adams, C. L., Polakis, P., Sellin, J. H. and Nelson, W. J. (1996). The adenomatous polyposis coli tumor suppressor protein localizes to plasma membrane sites involved in active cell migration. *J. Cell Biol.* **134**, 165-179.

Nicolson, T. (2005). Fishing for key players in mechanotransduction. *Trends Neurosci.* **28**, 140-144.

Noren, N. K., Niessen, C. M., Gumbiner, B. M. and Burridge, K. (2001). Cadherin engagement regulates Rho family GTPases. *J. Biol. Chem.* **276**, 33305-33308.

Novince, Z. M., Azodi, E., Marrs, J. A., Raymond, P. A. and Liu, Q. (2003). Cadherin expression in the inner ear of developing zebrafish. *Gene Expr. Patterns* **3**, 337-339.

O'Brien, L. E., Jou, T. S., Pollack, A. L., Zhang, Q., Hansen, S. H., Yurchenco, P. and Mostov, K. E. (2001). Rac1 orientates epithelial apical polarity through effects on basolateral laminin assembly. *Nat. Cell. Biol.* **3**, 831-838.

O'Brien, L. E., Zegers, M. M. and Mostov, K. E. (2002). Opinion: Building epithelial architecture: insights from three-dimensional culture models. *Nat. Rev. Mol. Cell. Biol.* **3**, 531-537.

Pollack, A. L., Barth, A. I., Altschuler, Y., Nelson, W. J. and Mostov, K. E. (1997). Dynamics of beta-catenin interactions with APC protein regulate epithelial tubulogenesis. *J. Cell Biol.* **137**, 1651-1662.

Radice, G. L., Rayburn, H., Matsunami, H., Knudsen, K. A., Takeichi, M. and Hynes, R. O. (1997). Developmental defects in mouse embryos lacking N-cadherin. *Dev. Biol.* **181**, 64-78.

Reifers, F., Bohli, H., Walsh, E. C., Crossley, P. H., Stainier, D. Y. and Brand, M. (1998). Fgf8 is mutated in zebrafish acerebellar (ace) mutants and is required for maintenance of midbrain-hindbrain boundary development and somitogenesis. *Development* **125**, 2381-2395.

Shimizu, T., Yabe, T., Muraoka, O., Yonemura, S., Aramaki, S., Hatta, K., Bae, Y. K., Nojima, H. and Hibi, M. (2005). E-cadherin is required for gastrulation cell movements in zebrafish. *Mech. Dev.* **122**, 747-763.

Sollner, C., Rauch, G. J., Siemens, J., Geisler, R., Schuster, S. C., Muller, U. and Nicolson, T. (2004). Mutations in cadherin 23 affect tip links in zebrafish sensory hair cells. *Nature* **428**, 955-999.

Suzuki, A. and Ohno, S. (2006). The PAR-aPKC system: lessons in polarity. *J. Cell Sci.* **119**, 979-987.

Troxell, M. L., Loftus, D. J., Nelson, W. J. and Marrs, J. A. (2001). Mutant cadherin affects epithelial morphogenesis and invasion, but not transformation. *J. Cell Sci.* **114**, 1237-1246.

Watanabe, T., Wang, S., Noritake, J., Sato, K., Fukata, M., Takefuji, M., Nakagawa, M., Izumi, N., Akiyama, T. and Kaibuchi, K. (2004). Interaction with IQGAP1 links APC to Rac1, Cdc42, and actin filaments during cell polarization and migration. *Dev. Cell* **7**, 871-883.

Waterman, R. E. and Bell, D. H. (1984). Epithelial fusion during early semicircular canal formation in the embryonic zebrafish, Brachydanio rerio. *Anat. Rec.* **210**, 101-114.

Westerfield, M. (2000). The Zebrafish Book. Eugene, OR: The University of Oregon Press.

Whitfield, T. T., Granato, M., van Eeden, F. J., Schach, U., Brand, M., Furutani-Seiki, M., Haffter, P., Hammerschmidt, M., Heisenberg, C. P., Jiang, Y. J. et al. (1996). Mutations affecting development of the zebrafish inner ear and lateral line. *Development* **123**, 241-254.

Whitfield, T. T., Riley, B. B., Chiang, M. Y. and Phillips, B. (2002). Development of the zebrafish inner ear. *Dev. Dyn.* **223**, 427-458.

Yu, W., Datta, A., Leroy, P., O'Brien, L. E., Mak, G., Jou, T. S., Matlin, K. S., Mostov, K. E. and Zegers, M. M. (2005). Beta1-integrin orients epithelial polarity via Rac1 and laminin. *Mol. Biol. Cell* **16**, 433-445.

Zegers, M. M., O'Brien, L. E., Yu, W., Datta, A. and Mostov, K. E. (2003). Epithelial polarity and tubulogenesis in vitro. *Trends Cell. Biol.* **13**, 169-176.